Design and Implementation of an Omnidirectional Spherical Robot *Omnicron*

Wei-Hsi Chen, Ching-Pei Chen, Wei-Shun Yu, Chang-Hao Lin, and Pei-Chun Lin

Abstract—**We report on a novel design and implementation of an omnidirectional spherical robot *Omnicron*. Instead of using wheels or flywheels, three omnidirectional wheels are installed inside the spherical shell and controlled independently; thus, the 3-degree-of-freedom planar omnidirectional mobility of the robot without any singularity condition can be achieved by simple forward 3-to-3 kinematic mapping. The performance of the robot is experimentally evaluated, thus proving its omnidirectional and trajectory-controllable mobility.**

I. Introduction

A spherical robot is a mobile robot with all its mechanism wrapped inside a spherical shell. Owing to its unique and intrinsic nature of geometrical symmetry, the robot is in principle capable of performing omnidirectional locomotion. However, because the robot can contact the ground in any configuration, the realization of omnidirectional locomotion is not trivial, and the design of driving mechanism should be addressed. According to the widely-used categorization, driving mechanism of the spherical robots can be divided into three categories: direct-driving, gravity, and angular momentum methods.

In the direct-driving method, the motor torque can be directly transmitted to the outer shell as the driving force for the robot. The concept was introduced in 1996 by Halme et al., where the robot had one active wheel and a steering joint mounted on the inside drive unit (IDU) with two points anchored to the outer shell [1]. In 1997, Bicchi et al. introduced the robot "Sphericle," where a small wheeled vehicle was placed within the outer shell [2]. In 2002, Michaud et al. introduced the robot "Roball" with a novel IDU which could be actively altered by changing the orientation of a heavy mass hanging on it, thus achieving the driving and steering functions [3]. Many researchers were inspired by this "gimbal mechanism-like" design, and this later became one of the mainstream design approaches for spherical robots. In 2004, Kabała et al. introduced "RoBall," the first spherical robot with an internal gimbal mechanism [4].

The second category is the gravity method. By manipulating the center of mass (COM) position of the robot,

a torque can be adequately created with respect to the ground contact point, thus driving the robot to roll. In 1999, Mukherjee et al. introduced "Spherobot," which had four movable masses moving on the four spokes extending from its geometrical center to the shell to generate desired rolling torque [5]. The concept was further analyzed by Javadi in the study for robot "Glory"[6]. The third category is the angular momentum method, which utilizes the characteristics of angular momentum conservation. In 2000, Bhattacharya et al. reported a robot design in this category [7]. In 2009, Jia et al. reported a spherical robot with only one orientation-changeable flywheel, achieving both driving and steering [8]. In 2008, Schroll introduced a "Gyrosphere robot," which combined the angular momentum (for driving) and gravity (for steering) methods [9].

One of the most important characteristics is the omnidirectional mobility since it is a unique feature of spherical robots. The planar coordinate system in general has three DOFs: forward/backward motion, lateral motion, and orientation. If a robot can perform these three types of motions at any instant, it is considered with omnidirectional mobility (i.e., hereafter referred to as "strict definition"). However, because the robot has symmetrical sphere, the orientation may not be crucial for spherical robots. Thus, in the "loose definition", the robot might be considered omnidirectional if it can perform forward/backward and lateral motions at any instant. In this sense, the robots using the gravity method can move omnidirectionally although its trajectory planning is challenging. Robots with flywheels can perform omnidirectional motion in most situations as well. However, such robots have certain singular configurations, which limit their movement to a certain direction. The similar situation of singularity occurs in robots with the gimbal-mechanism-based direct-driving method. In contrast, robots with the friction-based direct-driving method do not have a singularity problem. However, the wheels have nonholonomic constraints, so the robots cannot perform instant sharp turns (i.e., not omnidirectional). The characteristics of the robots with different configurations are summarized in fig. 1. The index "sharp turn" indicates that the robot is capable of performing sharp turn motions "at any position." However, change of motion direction may require a certain amount of time, so the locomotion with only sharp turn motion does not qualify as omnidirectional. In other words, the omnidirectional motion can be regarded as the

Authors are with Department of Mechanical Engineering, National Taiwan University (NTU), No.1 Roosevelt Rd. Sec.4, Taipei, Taiwan. (Corresponding email: peichunlin@ntu.edu.tw).
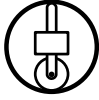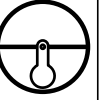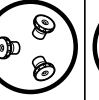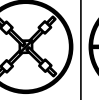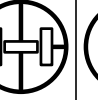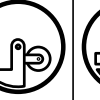
Robot Configuration	Single wheel	Hamster car	Pendulum on rotating axis	Gimbal mechanism	Single ball	Omni wheels	Mass movement	Orthogonally mounted flywheels	Flywheel on pendulum	Parallelly mounted flywheels
Driving mechanism	D	D	D		D	D	G	A	D/A	A/G
Input needed/ Output DOFs	2/2	⩾ 2/2	2/2		2/2	3/3	4/2	2/2	3/2	2/2
Sharp turn	V	V	V*		V	V	V	V*	V	
Omnidirectional locomation			V*		V	V	V	V*		

Fig. 1. Characteristics of the developed spherical robots. The symbols D, G, and A indicate direct-driving, gravity, and angular momentum methods, respectively. The mark "V" indicates the robot is capable of performing the specific motion, and the mark "V*" indicates the motion is achievable in most situations (i.e., with singularity). The method proposed in this paper is mentioned as the "Omni wheels."

capability of performing sharp turn motion "at any instant."

Previously, we have designed a spherical robot *OmniQiu* which uses direct-driving method and is capable of performing omnidirectional locomotion in the loose definition [10]. A small driven ball placed inside the spherical shell can be propelled to roll in any direction, so that this singularity-free robot can be driven omnidirectionally. However, owing to its single driving point, we found that the orientation of the inside mechanism may change, resulting in control difficulty of the overall robot locomotion. In this case, the third orientation DOF in the "strict definition" has its importance.

Here, with the desire of developing a spherical robot with full 3-DOF omnidirectional mobility, we report on a novel design of a spherical robot *Omnicron*. Instead of using a single driven ball as in *OmniQiu*, the robot utilizes three omnidirectional wheels to drive the spherical shell. Three wheels are controlled independently, thus achieving 3-DOF planar locomotion by simple 3 to 3 mapping. Among all the spherical robots, to the best of our knowledge, *Omnicron* is the only singularity-free omnidirectional robot with 3-DOF mobility.

The paper is organized as follows. The design concept of the spherical robot *Omnicron* is introduced in Section II, and forward and inverse kinematics of the robot is described in Section III. The implementation of the system and the performance evaluation are reported in Section IV. Section V concludes the work.

II. MECHANISM DESIGN

Design of *Omnicron* is set to meet the following specifications: (i) The robot uses the direct-driving method, which utilizes the motor power to directly drive the spherical robot via the transmission system; (ii) the robot is capable of performing 3-DOF omnidirectional locomotion. In order to generate continuous rolling motion of the shell, the mechanism inside the robot with the direct-driving method should have non-fixed contact points to the outer shell. Thus, the most widely-used method to satisfy this constraint is to install one or multi wheels inside the spherical shell. However, the fixed standard wheel ideally prevents the motion orthogonal to the rolling direction [11], thus impeding omnidirectional locomotion.

In order to generate 3-DOF omnidirectional mobility, at least three independently-controlled actuating mechanisms are needed. We caught our eyes on the omnidirectional wheels [12], which are widely used on the wheeled robot to achieve lateral and turn-in-place motions. Because small passive rollers are mounted on the wheel circumference with different rolling direction, the wheel can roll freely in the direction of the rollers. The direction of the roller in the 90-degree version during its ground contact is orthogonal to that of the wheel. Thus, the wheels can be driven to roll forward/backward on the surface with friction, and in the meantime, they don't give constraint to lateral motion and can be slid freely. In addition, by mounting three 90-degree omnidirectional wheels with rolling directions along with three sides of equilateral triangles, theoretically the system can perform 3-DOF omnidirectional motion. As a result, though the surface of the spherical shell is curvy, as long as the tangents of the ground contacts form the equilateral triangle, the simple and symmetric composition of the 3-DOF locomotion is still achievable. The final arrangement of *Omnicron* is shown in fig. 2, where three omnidirectional wheels are mounted according to the methodology described above.

In the sense of motion transmission, the robot can be separated into three parts, the spherical shell, the omnidirectional wheels, and the main body. The motors mounted on the body generate torques to roll the wheels, and rolling of the wheels further rolls the spherical shell. As a
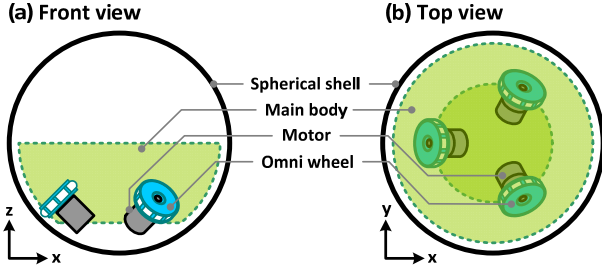
Fig. 2. Component arrangement of *Omnicron*.

Fig. 3. Illustrative diagram showing how wheel rotations compose the robot motion.

result, the whole robot is in motion. The amounts of rotations in all wheels determine the motion state of the overall robot. For example, as shown in fig. 3(a), for the robot motion along with x-axis, only two of the wheels rotate, with the same amounts. For the robot motion along with y-axis, as shown in fig. 3(b), all three wheels need to rotate with specific amounts, which will be described in detailed in the next section.

III. KINEMATICS MAPPING

The forward kinematics of *Omnicron* is composed of two mappings---mapping from motor speeds to the body motion, and then mapping from the body motion to the shell motion in the world frame (i.e., also the motion of the whole robot). To make the presentation clear, assume three principle axes of the main body are denoted as (X_b, Y_b, Z_b) as shown in fig. 4(a), and assume M_1, M_2, M_3 are the rotation axes of the motors viewing from the body frame. Though (M_1, M_2, M_3) are not mutually orthogonal to each other, they are still linearly independent and can span the whole $\mathbb{R}^3$ rotation space. In addition, assume (X, Y, Z) denote three principle axes of the world frame.

The mapping from the motor motion to the body frame can be found based on the phenomenon that angular velocity at every point of a rigid body remains the same [10]. Euler's Rotation Theorem reveals1` that an arbitrary rotation in three-dimensional space can be described by a single rotation φ along with certain fixed direction represented in a vector. In other words, any single rotation in three-dimensional space can be decomposed into three simultaneous rotations along with three principle axes of the body frame, referred to as simultaneous orthogonal rotations angles (SORA) [13]. Assume the angular velocity of the main body are denoted as $\Omega_B = (\omega_x, \omega_y, \omega_z)$ viewed from the body frame (X_b, Y_b, Z_b), and the angular speeds of the motors along with the directions (M_1, M_2, M_3) viewed from the body frame are $\Omega_M = (\omega_1, \omega_2, \omega_3)$, respectively. With the assumption of pure rolling between the wheels and the spherical shell, the relation between the motor speeds and the body angular speeds can be derived as
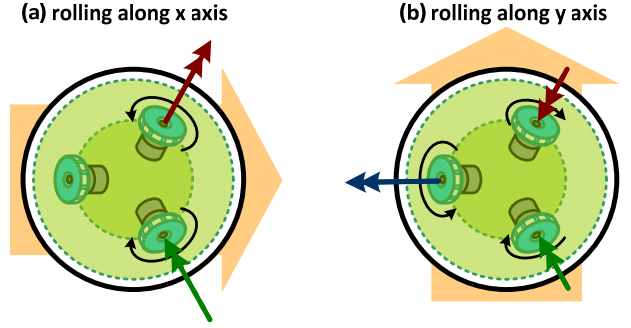
$$\omega_x = \frac{r_w}{r_s\sqrt{1-\cos^2\delta\cos^2\alpha}} \cdot \frac{1}{\cos\alpha}\omega_1 \tag{1}$$

$$= \frac{r_w}{r_s\sqrt{1-\cos^2\delta\cos^2\beta}} \cdot \frac{1}{\cos\beta}\omega_2$$

$$= \frac{r_w}{r_s\sin\delta} \cdot \frac{1}{\cos\gamma}\omega_3,$$

$$\omega_y = \frac{r_w}{r_s\sqrt{1-\cos^2\delta\sin^2\alpha}} \cdot \frac{1}{\sin\alpha}\omega_1 = \frac{r_w}{r_s\sqrt{1-\cos^2\delta\sin^2\beta}} \cdot \frac{1}{\sin\beta}\omega_2,$$

$$\omega_3 = 0,$$

$$\omega_z = \frac{r_w}{r_s\cos\delta}\omega_1 = \frac{r_w}{r_s\cos\delta}\omega_2 = \frac{r_w}{r_s\cos\delta}\omega_3$$

or equivalently,

$$\omega_1 = \frac{r_s}{r_w}[\sqrt{1-\cos^2\delta\cos^2\alpha} \cdot \cos\alpha \cdot \omega_x$$
$$+\sqrt{1-\cos^2\delta\sin^2\alpha} \cdot \sin\alpha \cdot \omega_y + \cos\delta \cdot \omega_z] \tag{2}$$
$$\omega_2 = \frac{r_s}{r_w}[\sqrt{1-\cos^2\delta\cos^2\beta} \cdot \cos\beta \cdot \omega_x$$
$$+\sqrt{1-\cos^2\delta\sin^2\beta} \cdot \sin\beta \cdot \omega_y + \cos\delta \cdot \omega_z]$$
$$\omega_2 = \frac{r_s}{r_w}[\sin\delta \cdot \cos\gamma \cdot \omega_x + \cos\delta \cdot \omega_z]$$

The equation shown above can further be reorganized into matrix form with notations Ω_M and Ω_B

$$\Omega_M = \frac{1}{n}A^{-1}\Omega_B$$

$$\begin{bmatrix} \omega_1 \\ \omega_2 \\ \omega_3 \end{bmatrix} = \frac{r_s}{r_w}\begin{bmatrix} \sqrt{1-\cos^2\delta\cos^2\alpha} \cdot \cos\alpha & \sqrt{1-\cos^2\delta\sin^2\alpha} \cdot \sin\alpha & \cos\delta \\ \sqrt{1-\cos^2\delta\cos^2\beta} \cdot \cos\beta & \sqrt{1-\cos^2\delta\sin^2\beta} \cdot \sin\beta & \cos\delta \\ \sin\delta \cdot \cos\gamma & 0 & \cos\delta \end{bmatrix}\begin{bmatrix} \omega_x \\ \omega_y \\ \omega_z \end{bmatrix}, \tag{3}$$

where $n = r_w/r_s$ is the ratio between the radius of the omnidirectional wheels r_w and the spherical shell r_s, and $(\alpha, \beta, \gamma, \delta)$ are configuration parameters of the motors with respect to the body frame as shown in fig. 4(b) and 4(c). Equation (2) represents the inverse kinematic mapping from the body motion Ω_B to the motor speed Ω_M. When $\alpha \neq \beta \neq \gamma$ and $\delta \neq 0$ (i.e., true in the configuration shown in fig. 4(a)), the matrix A^{-1} is at its full rank (i.e., $\det|A^{-1}| \neq 0$) and can be inversed. Thus, the forward kinematics can be derived as

$$\Omega_B = nA\Omega_M . \tag{4}$$

Assume the contact between the spherical shell and the ground is also pure rolling. If the main body remains horizontal during locomotion, the forward kinematic mapping from the body motion rotation Ω_B to 3 planar coordinates $V = (v_x, v_y, \omega_z)$ viewed from the world frame can be written as

$$V = R\Omega_B$$

$$\begin{bmatrix} v_x \\ v_y \\ \omega_z \end{bmatrix} = \begin{bmatrix} 0 & -r_s & 0 \\ r_s & 0 & 0 \\ 0 & 0 & 1 \end{bmatrix}\begin{bmatrix} \omega_x \\ \omega_y \\ \omega_z \end{bmatrix}, \tag{5}$$
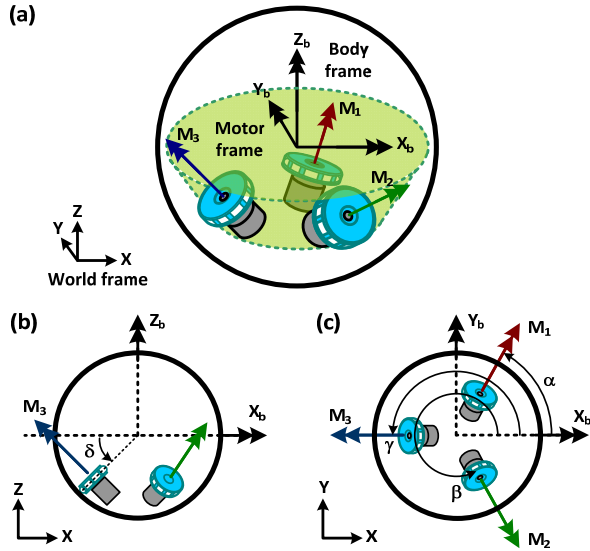
Fig. 4. Notations for kinematics.

where (v_x, v_y, ω_z) denote forward velocity , lateral velocity, and body orientation of the robot, respectively. Furthermore, the overall forward kinematic mapping from motor speeds Ω_M to the robot motion V can be represented as

$$V = nRA\Omega_M , \qquad (6)$$

and the inversed kinematic can be derived accordingly

$$\Omega_M = \frac{1}{n}A^{-1}R^{-1}V \qquad (7)$$

In reality, the main body tilts during locomotion. Thus, the mapping from the body frame to the robot motion shown in (5) requires some compensation. The body inclination can be represented in pitch and roll. In this case, in addition to R, the transformation matrix from the body coordinate to the world coordinate should include another a rotation matrix T which represents the inclination effect. Thus, the revised overall forward mapping becomes

$$V = RT\Omega_B = nRTA\Omega_M . \qquad (8)$$

Because the matrix A, R, and T are invertible, the overall inverse kinematics from the robot motion in the world frame to the motor speeds can now be written as

$$\Omega_M = \frac{1}{n}A^{-1}T^{-1}R^{-1}V . \qquad (9)$$

IV.   Performance Evaluation

Figure 5 shows the built platform to evaluate the performance of the proposed system, including the main body shown in 5(a), the main body installed inside the spherical shell shown in 5(b), and overall appearance shown in 5(c). The spherical shell is provided by a company which produces globes. The structure of the main body is constructed by the acrylic sheets because of their easy manufacturability by the laser cutter. The three 90-degree omnidirectional wheels are arranged in a configuration
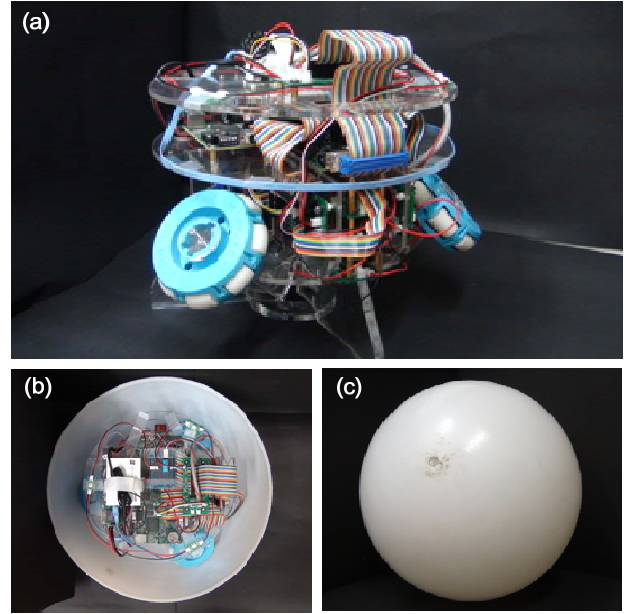

Fig. 5. The robot Omnicron: (a) the main body, (b) the body inside the spherical shell, and (c) the appearance.

Table I Robot specifications

Axis parameters	
Angle α	60º
Angle β	300º
Angle γ	180º
Angle δ	37.5º
Diameter	
Outer shell r_s	17 inch
Omni wheel r_w	4 inch
Weight	
Total	5,786 g
Shell	1,435 g
Main Body (without Omni wheels)	3,863.5 g
Omni Wheel	162.5 g/pc x3

shown in fig. 4(b) and 4(c), which satisfies $\alpha \neq \beta \neq \gamma$ and $\delta \neq 0$ to grant the inversibility of the matrices shown in section III. Table I lists the overall specifications of the spherical robot *Omnicron*. With this arrangement, the forward and inverse mappings from the motor speeds to the robot locomotion in the world frame can be successfully derived. The motors are controlled by a real time embedded control system (sbRIO-9642, National Instruments). Besides encoders for motor control, the robot has a 2-axis inclinometer (SCA100T, ±90º, VTI Technologies), which senses the body inclination with respect to gravity in real time.

The mobility of the robot was evaluated experimentally under various scenarios. A commercial HD camcorder (XDR-11, SONY) was placed on the ceiling to record the trajectories of the robot. LEDs are installed inside the spherical shell as the markers. The lighting of the LEDs significantly eases the followed post-processing in Matlab to

722

extract the positions of the markers from a sequence of images. The pitch and roll measured by the inclinometer are reported for analysis as well.

The locomotion of the robot was planned according to the following procedure. First, the routes were designed in the world frame (i.e., defining the dimensions of the circle and the square). Then, with the pre-set constant-speed robot motion, the trajectory was differentiated into velocity state since the kinematics was defined in this state as described in section III. Next, with the assumption of no body inclination during locomotion, the inversed kinematic shown in (7) were utilized to yield desired motor speeds. Finally, the velocity trajectories were integrated to yield position trajectories for position control. Empirical evaluation shows that the body indeed had small body inclination during locomotion. However, it is challenge to incorporate this variation into trajectory planning since the full body dynamics should be known as priori. On the other hand, the robot has encoders and the inclinometer, so the "empirical" preset trajectory can be computed after experiments. As shown in (8), by importing the encoder data and inclinometer into T and Ω_M, the "odometry" motion of the robot can be derived (hereafter this computed trajectory is referred to as the "empirical odometry").

A straight-line locomotion was performed as the baseline evaluation of the system. The robot was programmed to move 2 meters, and the experiments showed that the robot actually moved around 2.4 meters, 10% more than the set value. The percentage error might be acceptable owing to the complicate system behavior. Interestingly, the phenomenon was opposite to the general odometry behavior where the actual moving distance is in general less than the set distance owing to the ground slippage. We suspect that this phenomenon is the combined results of the motion inertia and the characteristics of the omnidirectional wheels in this particular setup. During the straight-line motion, the robot didn't move smoothly, but coupled move-and-swing motion was observed. When the robot started to move, firstly, the main body climbed up the spherical shell. Owing to the offset COM of the robot and motion inertia, the spherical shell
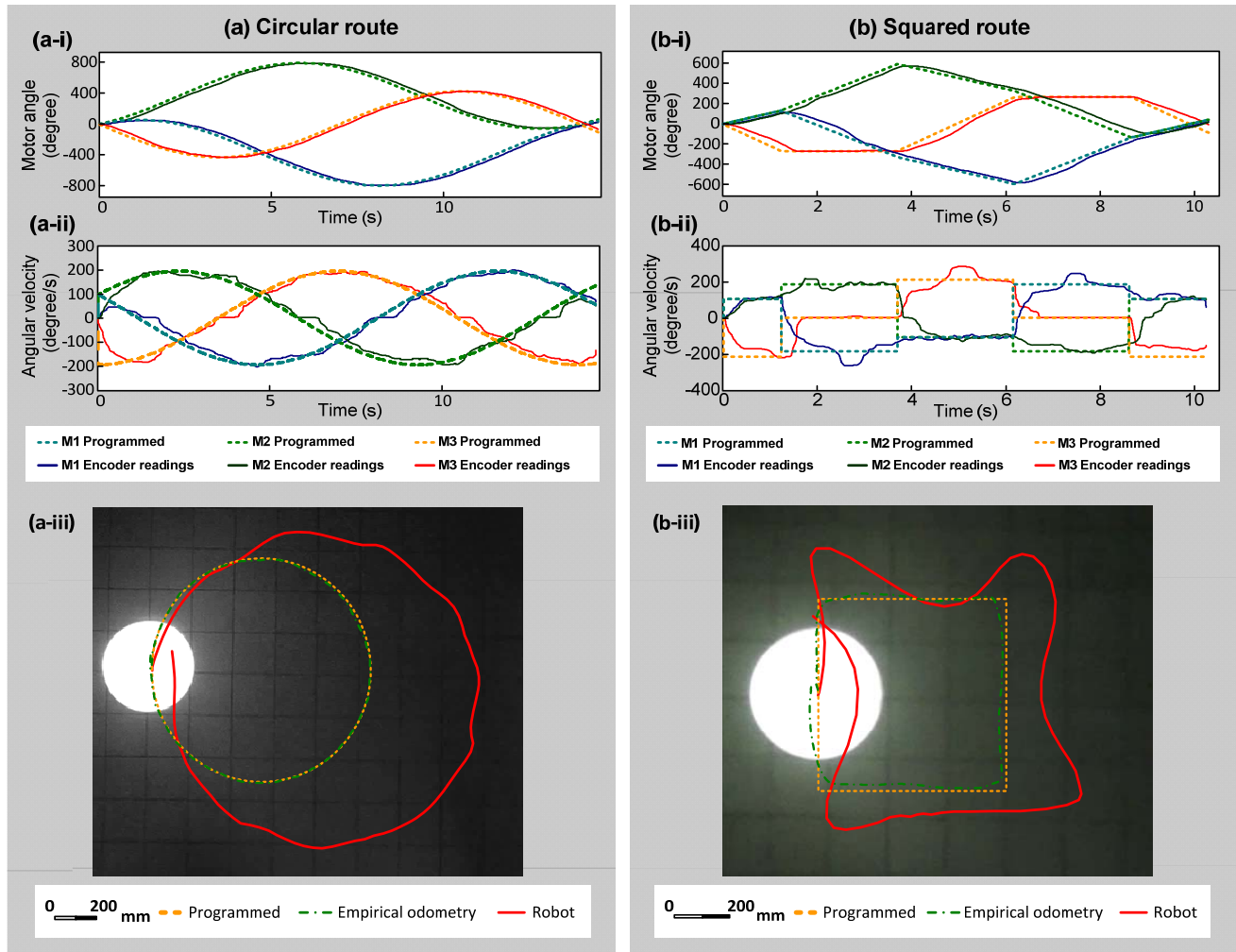

Fig. 6. Performance of the robot. The robot was programmed to move along with (a) a circular route and (b) a squared route, respectively. Subplots (-i) plot the programmed trajectories and the encoder readings. Subplots (-ii) plot the velocity state of the state shown in (-i). Subplots (-iii) plot the programmed trajectory, empirical odometry, and the robot trajectory, respectively.

started to roll. In the meantime, the climbed main body slid down within a speed higher than the wheel speeds. Once the forward torque to the shell was vanished, the main body again climbed up the shell and repeated the motion cycle. As a result, the overall locomotion of the robot in current setup is more like move-and-swing, but not continuous rolling. The climbing slippage was suspected to be less than the sliding slippage, so the robot moved more than predicted. A systematic study of body dynamics and its effect on the overall locomotion is under investigation.

Figure 6 shows the results of the robot moving in a circular route and a squared route, respectively. The subplots (a-i) and (b-i) plot the programmed trajectories and the encoder readings of three motors, where the dashed and solid lines represent the former and the latter, respectively. The subplots (a-ii) and (b-ii) plot the programmed and actual angular velocity. The actual curves were obtained by differentiating the encoder readings, thus the signals composed of high-frequency noise, but in general the trends of the trajectories matched the programmed ones. The subplots (a-iii) and (b-iii) show the programmed and empirical trajectories, where the yellow dotted lines, green solid lines, and red solid lines represent the programmed trajectory, empirical odometry, and the robot trajectory captured by the camera, respectively. The empirical odometry and the programmed trajectories are close to each other, which indicate that the body inclination only slightly affects the performance. The robot trajectories are larger than the other two trajectories. Similarly, we suspect this phenomenon is also resulted from the sliding as in the straight-line test. Though the actual circular route is 50% larger than the programmed one, the shape of the route indeed appears in the circular shape, which confirm the feasibility of performing planar locomotion. The sharp turning in the squared route induces certain dynamics effect, so the shape of the robot trajectory is not as close to the programmed one as in the circular case. The 3-dimensional dynamic model of the robot is under investigation to address this issue.

V. Conclusion

We report on the design and implementation of the novel omnidirectional spherical robot *Omnicron*. By installing three omnidirectional wheels inside the spherical shell, the robot is capable of performing 3-DOF omnidirectional locomotion by 3-to-3 mapping from the motor space to the robot locomotion in the world frame. The forward and inverse mappings are derived for trajectory planning and empirical trajectory investigation. The system is empirically built and evaluated in several scenarios, including motion along with a straight-line, a circular route, and a square route. The experimental results confirm that though not perfect, the

design concept is feasible and realistic, and the robot can indeed be operated to perform omnidirectional locomotion.

We are working on revising the robot with the goal of developing the robot's autonomous behavior. More specifically, we focus on deriving the 3-dimensional dynamic model of the robot, so the feedback controller can be implemented to yield smooth and accurate locomotion. In the meantime, we are also in the process of evaluating its mobility on rough terrain.

References

[1] A. Halme, T. Schönberg, and Y. Wang, "Motion control of a spherical mobile robot," in *Advanced Motion Control, 1996. AMC '96-MIE. Proceedings., 1996 4th International Workshop on*, 1996, pp. 259-264 vol.1.

[2] A. Bicchi, A. Balluchi, D. Prattichizzo, and A. Gorelli, "Introducing the "SPHERICLE": an experimental testbed for research and teaching in nonholonomy," in *Robotics and Automation, 1997. Proceedings., 1997 IEEE International Conference on*, 1997, pp. 2620-2625 vol.3.

[3] F. Michaud and S. Caron, "Roball, the rolling robot," *Autonomous Robots,* vol. 12, pp. 211-222, 2002.

[4] M. Kabała and M. Wnuk, "Design and construction of RoBall, a spherical, nonholonomic mobile robot," 2004.

[5] R. Mukherjee, M. A. Minor, and J. T. Pukrushpan, "Simple motion planning strategies for spherobot: a spherical mobile robot," in *Decision and Control, 1999. Proceedings of the 38th IEEE Conference on*, 1999, pp. 2132-2137 vol.3.

[6] A. H. J. A. and P. Mojabi, "Introducing Glory: A Novel Strategy for an Omnidirectional Spherical Rolling Robot," *Journal of Dynamic Systems, Measurement, and Control,* vol. 126, p. 678, 2004.

[7] S. Bhattacharya and S. K. Agrawal, "Spherical rolling robot: A design and motion planning studies," *Ieee Transactions on Robotics and Automation,* vol. 16, pp. 835-839, 2000.

[8] Q. Jia, Y. Zheng, H. Sun, H. Cao, and H. Li, "Motion control of a novel spherical robot equipped with a flywheel," in *Information and Automation, 2009. ICIA '09. International Conference on*, 2009, pp. 893-898.

[9] G. C. Schroll, "Design of a spherical vehicle with flywheel momentum storage for high torque capabilities," bachelor of science, Massachusetts Institute of Technology, Massachusetts Institute of Technology, 2008.

[10] W.-H. Chen, C.-P. Chen, J.-S. Tsai, J. Yang, and P.-C. Lin, "Design and Implementation of an Omnidirectional Spherical Robot," *Mechanism and Machine Theory,* 2012. (under review)

[11] R. Siegwart and I. R. Nourbakhsh, *Introduction to Autonomous Mobile Robots*: The MIT Press, 2004.

[12] M. Ashmore and N. Barnes, "Omni-drive Robot Motion on Curved Paths: The Fastest Path between Two Points Is Not a Straight-Line," in *AI 2002: Advances in Artificial Intelligence*. vol. 2557, B. McKay and J. Slaney, Eds., ed: Springer Berlin / Heidelberg, 2002, pp. 225-236.

[13] S. Tomažič and S. Stanči, "Simultaneous Orthogonal Rotations Angle," *Elektrotehniški vestnik - Journal of Electrical Engineering and Computer Science.,* 2011.